Lithos 258–259 (2016) 163–172

Contents lists available at ScienceDirect

Lithos

journal homepage: www.elsevier.com/locate/lithos

Using chalcophile elements to constrain crustal contamination and xenolith-magma interaction in Cenozoic basalts of eastern China

Gang Zeng [a,*], Xiao-Wen Huang [b], Mei-Fu Zhou [c], Li-Hui Chen [a], Xi-Sheng Xu [a]

[a] State Key Laboratory for Mineral Deposits Research, School of Earth Sciences and Engineering, Nanjing University, Xianlin Avenue 163, Nanjing 210046, China
[b] State Key Laboratory of Ore Deposit Geochemistry, Institute of Geochemistry, Chinese Academy of Sciences, Guiyang 550081, China
[c] Department of Earth Sciences, The University of Hong Kong, Hong Kong, China

ARTICLE INFO

Article history:
Received 25 February 2016
Accepted 29 April 2016
Available online 7 May 2016

Keywords:
Platinum-group elements
Alkaline basalts
Crustal contamination
Xenolith–magma interaction
Eastern China

ABSTRACT

Continental basalts have complicated petrogenetic processes, and their chemical compositions can be affected by multi-staged geological evolution. Compared to lithophile elements, chalcophile elements including Ni, platinum-group elements (PGEs) and Cu are sensitive to sulfide segregation and fractional crystallization during the evolution of mantle-derived magmas and can provide constraints on the genesis of continental basalts. Cenozoic intra-continental alkaline basalts in the Nanjing basaltic field, eastern China, include high-Ca and low-Ca varieties. All these basalts have poor PGE contents with Ir ranging from 0.016 ppb to 0.288 ppb and high Cu/Pd ratios from 0.7×10^5 to 4.7×10^5 (5.7×10^3 for DMM), indicating that they were derived from sulfide-saturated mantle sources with variable amounts of residual sulfide during melting or might undergo an early-sulfide segregation in the mantle. Relatively high Cu/Pd ratios along with high Pd concentrations for the high-Ca alkaline basalts indicate an additional removal of sulfide during magma ascent. Because these basalts have high, variable Pd/Ir ratios (2.8–16.8) with low Ce/Pb (9.9–19.7) ratios and ε_{Nd} values (+3.6–+6.4), crustal contamination is proposed to be a potential process to induce the sulfide saturation and removal. Significantly increased Pd/Ir ratios for few high-Ca basalts can be explained by the fractionation of laurite or Ru-Os-Ir alloys with olivine or chromite. For low-Ca alkaline basalts, their PGE contents are well correlated with the MgO, Sc contents, incompatible element ratios (Lu/Hf, Na/Ti and Ca/Al) and Hf isotopes. Good correlations are also observed between Pd/Ir (or Rh/Ir) and Na/Ti (or Ca/Al) ratios. Variations of these elemental ratios and Hf isotopes is previously documented to be induced by the mixing of peridotite xenolith-released melts during ascent. Therefore, we suggest that such xenolith–magma interaction are also responsible for the variable PGE compositions of low-Ca alkaline basalts.

1. Introduction

The origin of generally geochemical diversity of widespread intra-plate basalts remains a matter of considerable debate. In addition to fractional crystallization and differing degrees of partial melting, mantle source heterogeneity is an important factor on the geochemical compositions of such basalts, which is largely due to the recycling of crustal materials (e.g.Hofmann, 1997, 2003, Prytulak and Elliott, 2007, Willbold and Stracke, 2010). For continental basaltic magma, their chemical compositions can also be potentially modified by the contamination of crustal (Carlson et al., 1981; Koszowska et al., 2007) and/or lithospheric mantle components (Niu, 2008; O'Reilly and Zhang, 1995; Tang et al., 2006; Xu et al., 2005) during ascent. Therefore, the petrogenesis of continental basalts is complicated because their chemical compositions are generally affected by multiple processes. Platinum-group elements (PGEs) are extremely chalcophile and have extremely large partition coefficients between sulfide liquids and silicate magmas (e.g., Mungall and Brenan, 2014). Additonally, Os and Ir (IPGE) are more compatible in olivine and chromite, and Pt has strong affinities to native metals/alloys (see the review by Barnes et al., 2015). Compared to lithophile elements, PGEs of mantle-derived rocks are sensitive indicators of the extent of sulfide segregation. Both Ni and Cu are also chalcophile elements but Ni is more compatible and Cu incompatible during the magma evolution. Combined with Ni and Cu, PGEs are important for understanding the petrogenesis of continental basalts (e.g. Huang et al., 2013, Qi and Zhou, 2008, Wang et al., 2010).

Because these rocks have very low PGE contents and are difficult to obtain reliable PGE data, there are only sparse studies of PGEs in Cenozoic basalts in eastern China. Recent development of a modified digestion method for PGE (Qi et al., 2011) and the application of high-sensitivity ICP-MS make the determination of low-level PGE possible. Additionally, recent studies on some xenolith-rich intra-continental basalts suggest that the interaction between peridotite xenoliths and host basaltic magmas can modify the geochemistry of alkaline basalts (Lustrino et al., 2013; Zeng et al., 2013). Whether such xenolith–

* Corresponding author. Tel.: +86 25 89680895.
E-mail address: zgang@nju.edu.cn (G. Zeng).

http://dx.doi.org/10.1016/j.lithos.2016.04.032
0024-4937/

magma interaction can also affect the PGE compositions of basaltic magma needs to be evaluated. In this study, we report the PGE contents of some well-studied Cenozoic alkaline basalts from the Panshishan, Tashan, Guabushan, Fangshan (Luhe) and Fangshan (Jiangning) volcanoes in the Nanjing basaltic field. The aims of this study are to understand the behavior of PGEs during the formation and evolution of basaltic magmas and thus to constrain these processes. Together with major and trace element data, the new PGE dataset allow us to better understand the sulfide saturation and fractionation history of the magmas from which the basalts erupted.

The data presented here suggest that PGE compositions of alkaline basalts from Panshishan and Tashan volcanoes were modified during ascent by melts released from peridotite xenoliths, whereas those of basalts from the Guabushan, Luhe Fangshan and Jiangning Fangshan volcanoes were affected by crustal contamination.

2. Geological background

In eastern China, Cenozoic basalts are widely distributed along the coastal provinces and adjacent offshore shelf from north of Heilongjiang province to south of Hainan island (Fig. 1a), which constitute the eastern China volcanic belt. In general, volcanic activity in eastern China is associated closely with the major regional faults. The research area, the Nanjing basaltic field, is located in the central part of eastern China, east of the Tan-Lu Fault (Fig. 1a). The central part of eastern China is characterized by the Dabie–Sulu orogenic belt (Fig. 1a), which is a Triassic collision zone between the North China and Yangtze cratons (Li et al., 1999; Zheng et al., 2003; Zheng et al., 2005). The Cenozoic basalts in this area were predominantly emplaced and erupted between Paleocene and Miocene (Liu et al., 1992), and were extensive and widespread near the Tan-Lu Fault, with lava flows covering an area of over 1000 km^2 (Fig. 1b). The eruption of volcanoes formed mainly alkali olivine basalts and tholeiites in this region. In the region distal from the Tan-Lu Fault, the basalts are associated with small isolated volcanoes, and their lithologies are generally alkali olivine basalts with minor basanites/tephrites.

3. Petrography

Basalts from Panshishan and Tashan belong to low-Ca alkaline basalts, whereas those from Guabushan, Luhe Fangshan and Jiangning Fangshan are high-Ca alkaline basalts (Zeng et al., 2013).

All low-Ca alkaline basalts are dark to dark gray and massive. They are typically fresh and contain variable amounts of olivine phenocrysts (<10% modal abundance) set in a groundmass of olivine, Ti-magnetite, plagioclase, and glass. There is a lack of pyroxene or plagioclase phenocrysts. Few olivine xenocrysts (<1% modal abundance for most samples) can also be observed in these basalts. Additionally, they contain abundant peridotite xenoliths up to 50–80 vol% in some outcrops. These xenoliths usually have distinct cores and margins (Fig. 1c). Clinopyroxene within xenolith cores is typically zoned with non-spongy cores and sponge-textured margins, whereas clinopyroxene within xenolith margins does not have obvious zoning but show sponge textures throughout the entire crystal. In addition, the margin of xenolith contains more olivine and less orthopyroxene than the core of the

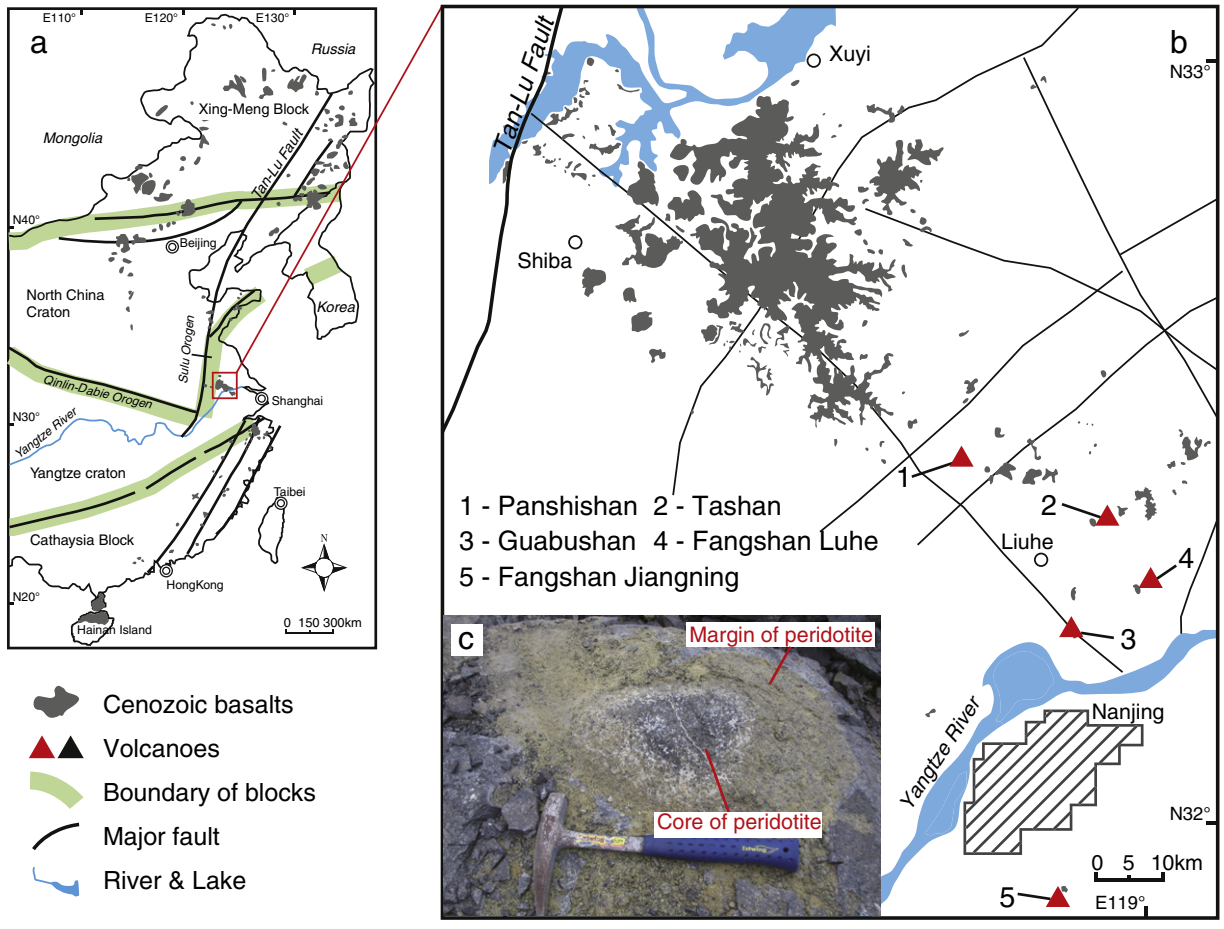

Fig. 1. (a) Simplified geological map of eastern China. Distributions of Cenozoic basalts in eastern China are after Liu et al. (1992). (b) Distribution of Cenozoic basalts in Nanjing basaltic field, central eastern China. Distributions of Cenozoic basalts and major faults in this area are based on Anhui Institute of Geological Survey (1977); Jiangsu Institute of Geological Survey (1978), and Zhao et al. (1983). (c) Photograph for peridotite xenolith hosted in Tashan basalts (Zeng et al., 2013).

xenolith, and some orthopyroxenes are enclosed in the olivines at the margin. Crustal xenolith fragments are rare or absent in these samples.

High-Ca basalts from the Guabushan and Luhe Fangshan volcanoes are dark, dark gray, or light gray, whereas samples from the Jiangning Fangshan are dark red. High-Ca alkaline basalts are massive with minor basalts from the Luhe Fangshan volcano with vesicular or amygdaloidal structure. In general, high-Ca alkaline basalts are fresh. The samples from the Jiangning Fangshan volcano are slightly altered, for instance, olivine phenocrysts are partially altered to low-temperature iddingsite. Few basalts from the Luhe Fangshan volcano show cryptocrystalline, equigranular and intergranular textures. Other high-Ca alkaline basalts are porphyritic and composed of minor olivine phenocrysts (<10% modal abundance) set in a groundmass of olivine, Ti-magnetite, plagioclase, and volcanic glass; neither pyroxene nor plagioclase phenocrysts are observed in these samples. Few olivine xenocrysts (<1% modal abundance) can also been observed in the Guabushan basalts. Mantle xenoliths and crustal xenolith fragments can be observed in some samples from the Luhe Fangshan volcano.

4. Analytical methods

4.1. Whole-rock major and trace elements

Whole-rock major elements were determined at the State Key Laboratory for Mineral Deposits Research, Nanjing University, China, using a Thermo Scientific ARL 9900 X-ray fluorescence spectrometer (XRF). According to the measured values of the rock reference material (GSR3), the uncertainties are less than 2% for Si, Ti, Al, Fe, Mg and Ca, and less than 6% for Mn, K, Na and P.

Whole-rock trace elements were analyzed at the Department of Geology, Northwest University, China, using an ELAN 6100 DRC inductively coupled plasma mass spectrometer (ICP-MS) after acid digestion ($HF + HNO_3$) of samples in sealed Teflon bombs. The analyses of USGS rock reference materials (BHVO-2 and BCR-2) yield precisions better than 5% for Sc, V, Cr, Co, Ni, Rb, Sr, Y, Zr, Nb, Ta, Cs, Ba, Pb and REEs, and 10% for U and Th.

4.2. Nd–Hf isotopes

Nd isotopic analyses were performed using a Finnigan Triton TI thermal ionization mass spectrometer at the State Key Laboratory for Mineral Deposits Research, Nanjing University. Detailed analytical procedures for Nd isotopic measurements are described in Pu et al. (2005). The Nd isotopic compositions were normalized to $^{146}Nd/^{144}Nd = 0.7219$. Measured $^{143}Nd/^{144}Nd$ value of standard JNdi-1 was 0.512120 ± 0.000004, which is in agreement with the average $^{143}Nd/^{144}Nd$ value of 0.512102 ± 0.000022 ($n = 50$, 2σ) during one-year measurement.

Hf isotopic compositions were obtained using a Neptune plus (Thermo Fisher Scientific) multi-collector inductively coupled plasma mass spectrometer (MC-ICP-MS) at the Institute of Geology and Geophysics, Chinese Academy of Sciences. Detailed chemical separation procedures for Hf isotopic measurements are given by Yang et al. (2010). The Hf isotopic compositions were normalized to $^{179}Hf/^{177}Hf = 0.7325$. Reference material BHVO-2 was analyzed as the unknown sample, and the measured value was 0.283106 ± 0.000006 for $^{176}Hf/^{177}Hf$, which is in agreement with the reference values of 0.283105 ± 0.000011 (Weis et al., 2007).

4.3. Whole-rock platinum group elements

To avoid the potential influence of peridotite fragments, before crushing the samples into powder, all samples are firstly crushed into fragments with a size of 3~5 mm, and then the peridotite fragments are ruled out as far as possible. Whole-rock PGEs were determined by isotope dilution (ID)-ICPMS using a modified digestion method (Qi et al., 2011) at the State Key Laboratory of Ore Deposit Geochemistry, Institute of Geochemistry, Chinese Academy of Sciences. Five grams of rock powder and appropriate amounts of the enriched isotope spike solution ^{101}Ru, ^{193}Ir, ^{105}Pd and ^{194}Pt were weighed and placed in a 120 ml PTFE beaker. About 5 ml of water was added to wet the sample and then 25 ml of HF was added slowly. The solutions were evaporated to dryness to remove silicates. 5 ml of HF and 15 ml of HNO_3 were then added. After heating the sealed bombs at 190 °C for 24 h, the solutions were evaporated to dryness and concentrated HCl was added. After drying, the solutions were conditioned to 2 N HCl and transferred to 50 ml centrifuge tubes. After centrifuging, the supernatant was transferred to the original beaker and used to preconcentrate PGE by Te-coprecipitation. The main interfering elements, such as Cu, Ni, Zr and Hf, were removed by a mixed ion exchange column that contained a Dowex 50W-X8 cation exchange resin and a P507 levextrel resin.

All PGEs were determined by a PE Elan DRC-e ICP-MS. Iridium, Ru, Pt and Pd were measured with isotope dilution and the content of Rh was calculated using ^{194}Pt as an internal standard (Qi et al., 2004). The analytical results for the standard reference materials, WGB-1 (gabbro) and TDB-1 (diabase), are in good agreement with the certified values (Table 1). The total procedural blanks were lower than 0.002 ng for Ru, Rh and Ir, and 0.006 ng for Pt and Pd.

Table 1
PGE compositions (10^{-9}) of Cenozoic alkaline basalts and peridotite xenoliths in the Nanjing basaltic field and reference materials.

Elements	Ir	Ru	Rh	Pt	Pd	Pd/Ir	Rh/Ir
High-Ca alkaline basalts							
08GPS03	0.031	0.087	0.016	0.372	0.397	12.93	0.52
08GPS07	0.022	0.067	0.019	0.294	0.369	16.83	0.85
08FSJN00	0.020	0.064	0.017	0.242	0.243	12.42	0.88
08FSJN01	0.019	0.058	0.020	0.225	0.206	11.14	1.07
08FSJN02	0.024	0.077	0.025	0.221	0.231	9.75	1.05
08FSJN03	0.016	0.066	0.019	0.266	0.144	9.08	1.17
08FSJN04	0.017	0.056	0.014	0.176	0.161	9.51	0.82
08FSJN06	0.017	0.060	0.012	0.192	0.138	8.30	0.74
08FSLH03	0.060	0.242	0.057	0.411	0.290	4.84	0.95
08FSLH04	0.041	0.104	0.021	0.225	0.306	7.46	0.52
08FSLH06	0.059	0.140	0.039	0.359	0.519	8.80	0.66
08FSLH10	0.033	0.058	0.018	0.232	0.234	7.10	0.55
08FSLH14	0.048	0.072	0.025	0.216	0.263	5.47	0.52
08FSLH16	0.288	0.522	0.169	0.779	0.816	2.83	0.59
08FSLH17	0.269	0.526	0.147	0.742	0.820	3.05	0.55
Low-Ca alkaline basalts							
08PSS01	0.030	0.056	0.081	0.115	0.163	5.41	2.67
08PSS02	0.118	0.278	0.064	0.423	0.361	3.05	0.54
08PSS04	0.082	0.263	0.070	0.411	0.274	3.34	0.85
08PSS05	0.142	0.404	0.091	0.550	0.507	3.58	0.64
08PSS06	0.076	0.204	0.062	0.384	0.437	5.77	0.83
08PSS07	0.159	0.311	0.067	0.329	0.396	2.49	0.42
08PSS08	0.127	0.262	0.059	0.352	0.400	3.14	0.46
08TS03	0.167	0.392	0.124	0.898	0.475	2.84	0.74
08TS05	0.195	0.301	0.122	0.343	0.361	1.85	0.63
Core of Peridotite xenolith in low-Ca alkaline basalts							
14PSS-X01	4.056	7.882	1.054	4.732	4.268	1.05	0.26
14TS-X02	3.601	5.865	1.075	4.952	4.092	1.14	0.30
14TS-X04	3.666	5.808	1.388	5.540	5.123	1.40	0.38
Margin of Peridotite xenolith in low-Ca alkaline basalts							
14TS-X03	4.153	6.878	1.295	6.084	4.640	1.12	0.31
14PSS-X02	4.626	7.488	1.232	5.297	4.146	0.90	0.27
14TS-X01	3.846	6.514	1.205	5.901	4.653	1.21	0.31
Reference material WGB-1 (gabbro)							
This study	0.250	0.240	0.360	6.050	13.400		
1σ	0.080	0.050	0.010	0.480	0.500		
Meisel and Moser (2004)	0.211	0.144	0.234	6.390	13.900		
Govindaraju (1994)	0.330	0.300	0.320	6.100	13.900		
Reference material TDB-1 (diabase)							
This study	0.087	0.310	0.450	5.050	21.000		
1σ	0.033	0.010	0.060	0.220	1.200		
Meisel and Moser (2004)	0.075	0.198	0.471	5.010	24.300		
Govindaraju (1994)	0.150	0.300	0.700	5.800	22.400		

5. Analytical results

5.1. Major and trace elements and Nd–Hf isotopes

Major and trace element and Nd–Hf isotope compositions of high-Ca alkaline basalts are reported in Table S1. The major element, trace element and Hf isotope compositions of low-Ca alkaline basalts are from Zeng et al. (2013).

Elemental and Nd–Hf isotopic compositions of low-Ca alkaline basalts have been presented in a previous study (Zeng et al., 2013), and are briefly summarized here. Low-Ca alkaline basalts contain medium to high SiO_2 (46.5–52.3 wt.%) concentrations, high total alkali ($Na_2O + K_2O$ = 6.0–11.6 wt.%) and Al_2O_3 (14.1–17.4 wt.%) contents, low to medium concentrations of MgO (1.8–9.5 wt.%), low TiO_2 (0.8–1.9 wt.%) and CaO (4.1–7.8 wt.%) concentrations, and low Ca/Al (0.3–0.6) and high Na/Ti (2.8–11.2) ratios. These basalts have obvious correlations between MgO and other oxides (CaO, $Fe_2O_3^T$, K_2O, and Al_2O_3). Compatible elements (Ni, Cr, and Sc) of low-Ca alkaline basalts positively correlate with MgO, whereas incompatible elements (Rb and Hf) negatively correlate with MgO. In addition, these basalts are light rare earth element (LREE)-enriched (La/Yb = 34.0–98.5). In the primitive-mantle normalized incompatible element diagram, these basalts have patterns similar to OIBs with Nb and Ta enrichment and Pb depletion relative to the LREE. The low-Ca alkaline basalts show limited ranges in Nd and Hf isotopic compositions (ε_{Nd} = 6.8–7.4, ε_{Hf} = 9.5–13.0). Small-scale but systematic changes in Hf isotopic compositions along with variable elemental ratios (Ca/Al, Ti/Ti*, and Lu/Hf ratios) are present for the Panshishan basalts.

Compared to low-Ca alkaline basalts, high-Ca alkaline basalts contain relatively low concentrations of total alkali ($Na_2O + K_2O$ = 4.8–5.8 wt.%) and Al_2O_3 (13.7–16.0 wt.%), high concentrations of MgO (4.3–10.0 wt.%), TiO_2 (1.5–2.4 wt.%) and CaO (7.0–8.6 wt.%), and high Ca/Al (0.6–0.8) and low Na/Ti (1.2–1.8) ratios. The Ni and Cr of high-Ca alkaline basalts are positively correlated with MgO (Fig. 2). High-Ca alkaline basalts have smooth chondrite-normalized REE patterns without Eu or Ce anomalies and show lower LREE/ HREE ratios (La/Yb = 10.2–23.2) than low-Ca alkaline basalts. In a primitive-mantle normalized incompatible element diagram, high-Ca alkaline basalts have patterns generally similar to those of low-Ca alkaline basalts, but with less Pb and Ti anomalies. Furthermore, high-Ca alkaline basalts have more enriched isotopic compositions (ε_{Nd} = +3.6–+6.4, ε_{Hf} = +7.9–+10.5) than low-Ca alkaline basalts.

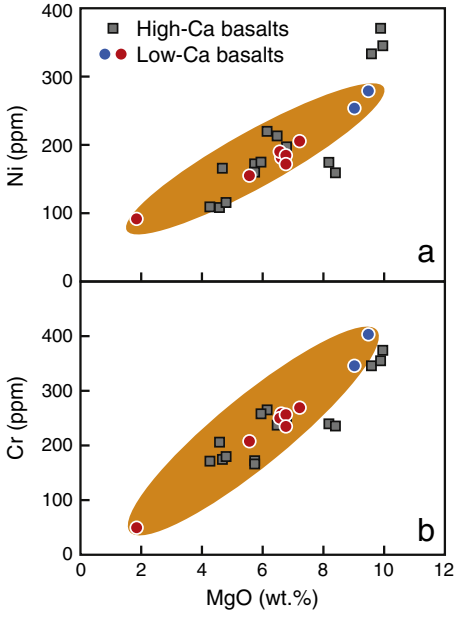

Fig. 2. Variations in Ni (a) and Cr (b) vs. MgO for Cenozoic alkaline basalts in Nanjing basaltic field. Red circles and blue circles stand for low-Ca alkaline basalts from the Panshishan and Tashan volcanoes, respectively. Gray squares stand for high-Ca alkaline basalts from the Guabushan, Luhe Fangshan and Jiangning Fangshan volcanoes.

5.2. Chalcophile elements

PGE compositions of low-Ca alkaline basalts, high-Ca alkaline basalts and peridotite xenoliths of the Panshishan and Tashan volcanoes are reported in Table 1.

Low-Ca alkaline basalts have highly variable PGE concentrations with Ir ranging from 0.030 to 0.195 ppb. PGE concentrations are generally positively correlated to MgO contents (Fig. 3). In addition, correlations can also be observed in the plots of the PGE compositions vs. Sc concentrations, Hf isotopes and some element ratios (Lu/Hf, Na/Ti and Ca/Al) (Figs. 4, 5). With the decreased Ir or Pd concentrations, low-Ca alkaline basalts have decreased Sc concentrations, increased ε_{Hf} values, decreased Lu/Hf and Ca/Al ratios, and increased Na/Ti ratios. In the primitive mantle-normalized chalcophile element patterns (Fig. 6a), these basalts are depleted in PGE relative to Ni and Cu, but show positive anomalies of Rh. PPGE (Rh, Pd and Pt) are slightly richer than IPGE (Ir and Ru) with Pd/Ir ratios from 1.85 to 5.77. Their Cu/Pd ratios (0.7×10^5–1.3×10^5) are relatively constant.

Most high-Ca alkaline basalts, except samples 08FSLH16 and 08FSLH17, are also poor in PGE, especially Ir, Ru and Rh (Ir = 0.016–0.060 ppb). However, samples 08FSLH16 and 08FSLH17 show obviously higher PGE contents than other high-Ca alkaline basalts (Ir = 0.269–0.288 ppb). The PGE concentrations of high-Ca alkaline basalts are poorly correlated with MgO and Sc concentrations, Hf isotopes, and element ratios (Figs. 3, 4, 5). In a primitive mantle-normalized chalcophile element diagram, all high-Ca alkaline basalts are depleted in PGE relative to Ni and Cu (Fig. 6b). They show more remarkable fractionation between IPGE and PPGE (Pd/Ir = 2.83–16.83) than low-Ca alkaline basalts. Furthermore, Pd/Ir and Cu/Pd ratios (0.7×10^5–4.7×10^5) of high-Ca alkaline basalts are highly variable, and the Pd/Ir ratios of most samples are negatively correlated with their Ce/Pb ratios and Nd isotopes (Fig. 7).

Peridotite xenoliths hosted in low-Ca alkaline basalts have higher PGEs than the host rocks, with limited variations (Ir = 3.601–4.626 ppb). Both the cores and margins of peridotites have similar PGE concentrations, with 3.601–4.056 ppb Ir and 3.846–4.626 ppb Ir, respectively. In a primitive-mantle-normalized chalcophile element diagram, peridotite xenoliths show relatively flat PGE patterns with slightly negative Pt anomalies (Fig. 6c).

6. Discussion

6.1. Fractional crystallization

Decreased MgO, Ni and Cr concentrations of low-Ca alkaline basalts from Nanjing may initially be thought to be related to the fractional crystallization of silicates (e.g., olivine). However, the presence of abundant mantle xenoliths (5–80 cm diameter) in these basalts suggests that these alkaline magmas ascended rapidly and seem to have no time to undergo fractional crystallization (Zeng et al., 2013). Additionally, small-scale but systematic changes in Hf isotopic compositions along with variable Lu/Hf ratios are presented within the low-Ca alkaline basalts from the Panshishan volcano (Zeng et al., 2013), which cannot be explained by fractional crystallization. The correlations between PGE compositions and Hf isotopes (or Lu/Hf ratios) (Figs. 4, 5) also indicate that the PGE compositions of low-Ca alkaline basalts are not affected by the fractionation process of silicates.

For high-Ca alkaline basalts, Ni and Cr contents are well correlated with MgO contents (Fig. 2), which can be explained by the fractional crystallization of olivine or chromite. Poor correlation between MgO

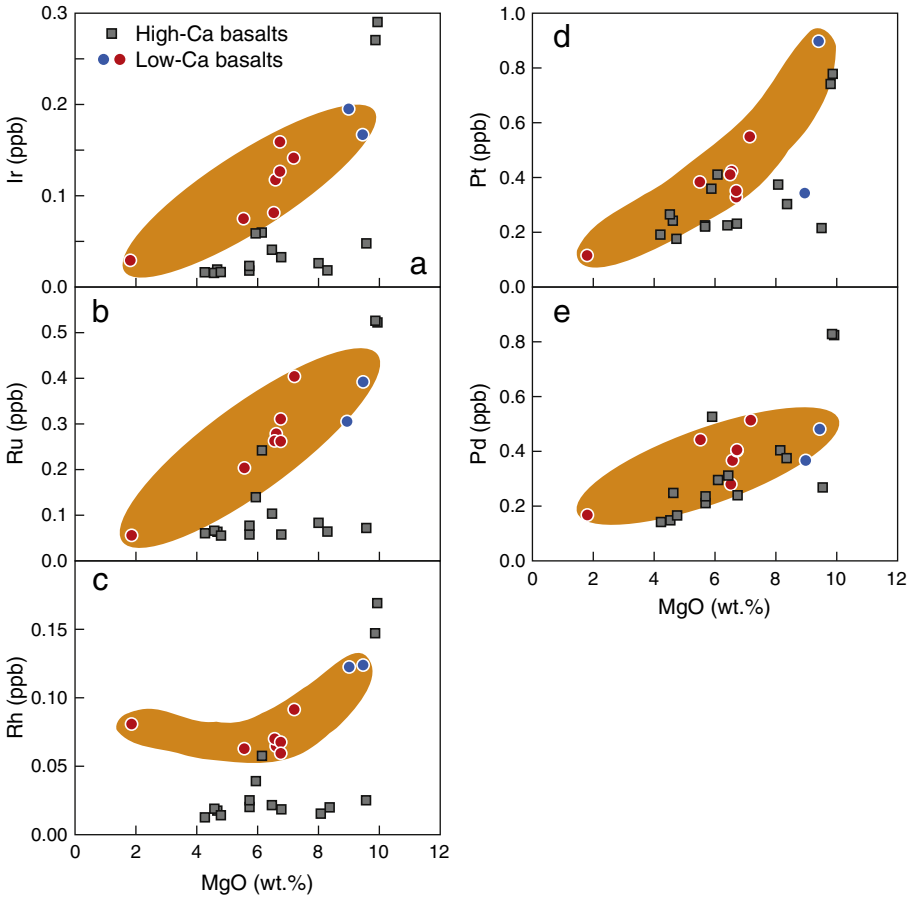

Fig. 3. Variations in PGEs vs. MgO for Cenozoic alkaline basalts in the Nanjing basaltic field.

and CaO (or Sc), and high CaO (7.0–8.6 wt.%) and Sc (16.4–23.6 ppm) contents indicate negligible fractional crystallization of pyroxenes for high-Ca alkaline basalts. Lack of negative Eu anomalies for these basalts (not shown) indicates no significant removal of plagioclase. However, high-Ca basalts show poor correlations between PGEs and MgO contents, indicating that the fractionation of olivine or chromite is not the unique factor to affect their PGE compositions, and more geological processes should be considered.

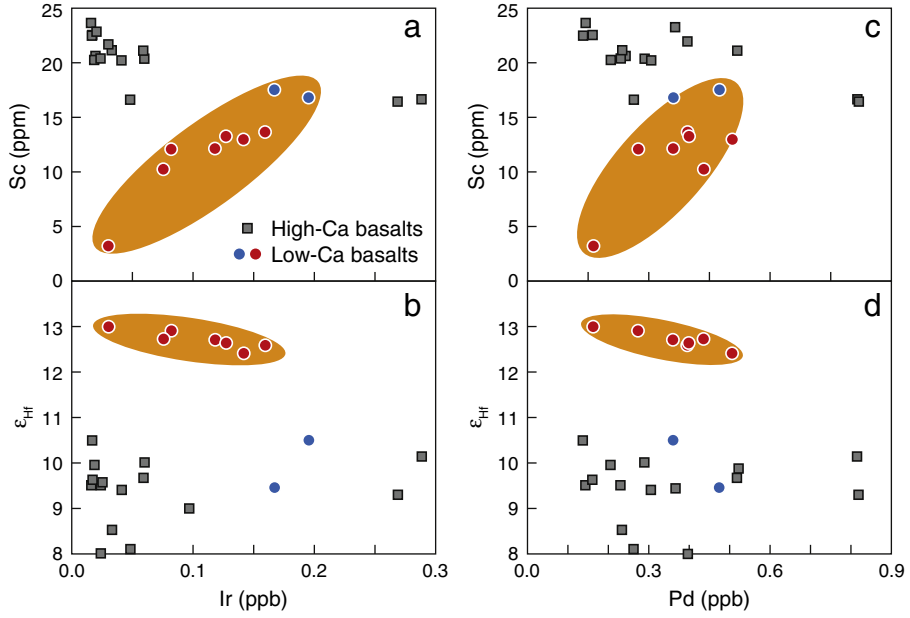

Fig. 4. Variations in Sc vs. Ir (a), ε_{Hf} vs. Ir (b), Sc vs. Pd (c), and ε_{Hf} vs. Pd (d) for Cenozoic alkaline basalts in Nanjing basaltic field.

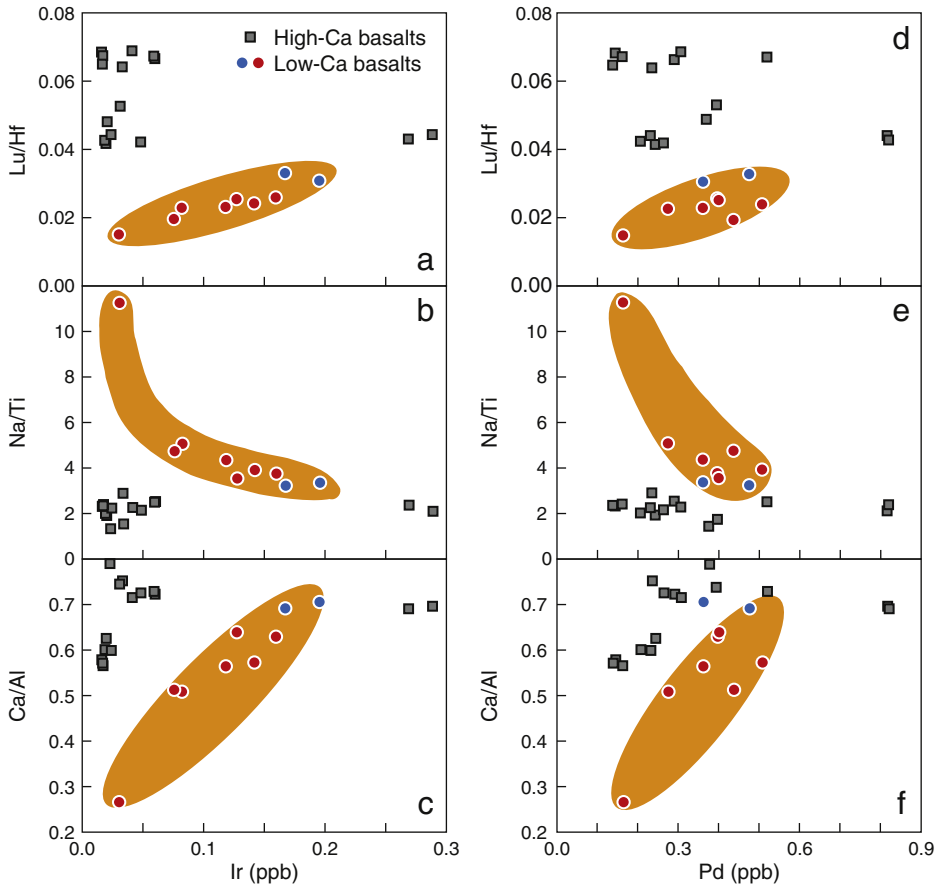

Fig. 5. Variations in incompatible element ratios (Lu/Hf, Na/Ti and Ca/Al) vs. Ir (a, b, c) and Pd (d, e, f) for Cenozoic alkaline basalts in the Nanjing basaltic field.

6.2. Partial melting

The low HREE concentrations of alkaline basalts in the Nanjing basaltic field (Yb = 1.3–1.9 ppm) suggest that they derive dominantly from a garnet-facies mantle because garnet has high HREE partition coefficients (e.g., Klemme et al., 2002). The Sm/Yb ratios in basalts will also descend with increasing degrees of partial melting if garnet is residual in the source; therefore, the Sm/Yb ratios can potentially be used to reflect variations in the degree of partial melting. Based on the Sm/Yb and La/Yb ratios of these alkaline basalts, we calculated their partial melting degrees in previous studies (Zeng et al., 2013). The estimated partial melting degrees of high-Ca alkaline basalts (8%–20%) are higher than those of low-Ca alkaline basalts (2%–6%). Such estimates are consistent with the differing contents of incompatible elements (e.g., Nb, Th, La, and Nd) between low-Ca (Nb = 75–170 ppm; La = 49–138 ppm) and high-Ca (Nb = 27–72 ppm; La = 13–42 ppm) alkaline basalts, because the concentrations of incompatible elements in basaltic melts increases with decreasing degree of melting.

Partial melting in different degrees can also modify the PGE compositions of basaltic magmas. It has been suggested that high IPGE with low Pd/Ir ratios of magma are produced by relatively high degrees of partial melting, e.g., komatiites in Zimbabwe (Zhou, 1994) and basalts in Deccan Traps (Crocket and Paul, 2004). However, high-Ca alkaline basalts, which have undergone higher degree of partial melting (8%–20%) than low-Ca alkaline basalts (2%–6%), show higher Pd/Ir ratios (2.8–16.8) than low-Ca alkaline basalts (1.9–5.8). Obviously, the variation of PGE compositions of these alkaline basalts are not mainly controlled by different partial melting degree.

6.3. Depletion of PGEs related to sulfide segregation in the source region

The retention of sulfides during partial melting of mantle is also a critical control on PGE contents of the basaltic melts. If the mantle source is sulfide-saturated, then the residue of sulfide, even tiny amounts, in the source can induce strong PGE depletion in basaltic melts because of high partition coefficients for PGE between sulfide and silicate melt (e.g., D^{Ir} = 4400–1,900,000, D^{Pd} = 6300–536,000) (Bezmen et al., 1994; Mungall and Brenan, 2014; Peach et al., 1994). In comparison, melting of sulfur under saturated mantle is suggested to produce PGE-enriched (especially PPGE) magmas (Seitz and Keays, 1997). However, the sulfide-saturated mantle source can also produce PGE-enriched basaltic magmas if the melting degree is sufficiently high to remove the entire source sulfide by dissolving it in the melt. In this condition, at least 25% of partial melting is required (Keays, 1995; Momme et al., 2003; Rehkamper et al., 1999). Significant PGE depletion for these alkaline basalts in Nanjing basaltic field (Fig. 3) indicates that their mantle source is sulfide-saturated. The estimated partial melting degrees of high-Ca (8%–20%) and low-Ca (2%–6%) alkaline basalts are lower than 25%, which also support that the residual sulfides cannot be consumed absolutely. Furthermore, recent studies on Hawaiian picrate (Bennett et al., 2000) suggest that if the sulfide is retained in the mantel source, the picrate should have high, constant Cu/Pd ratios (on a log scale) with variable Cu contents. A similar phenomenon can also be observed in the Nanjing basalts. Their Cu contents range from 15 ppm to 65 ppm, while most samples show relatively high and constant Cu/Pd ratios (0.7×10^5–1.2×10^5).

To evaluate whether the depletion of PGEs is induced by the residue of sulfide in the mantle source, we also performed modeling of mantle melting in the plots of Cu/Pd vs. Pd (Fig. 8). Because partition coefficient

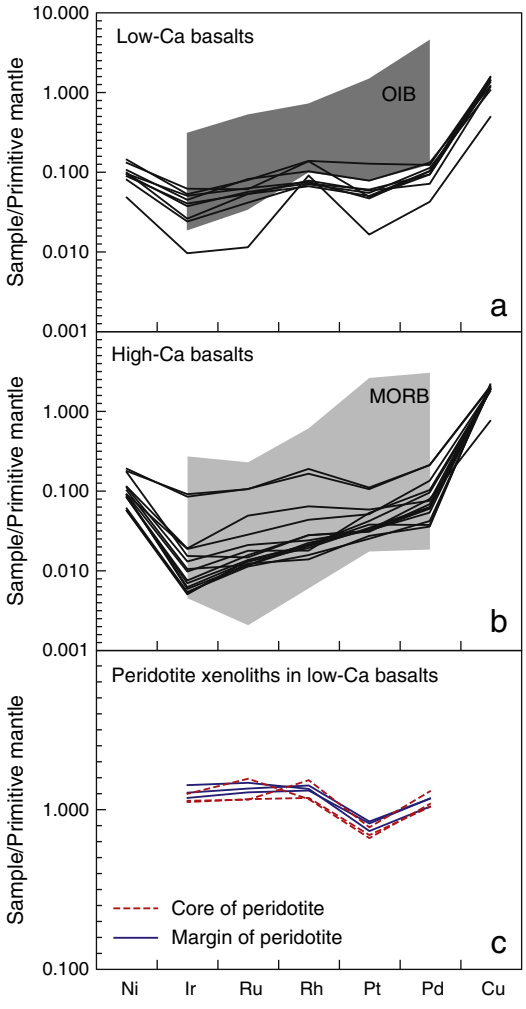

Fig. 6. Primitive-mantle-normalized chalcophile element diagram for Cenozoic low-Ca alkaline basalts (a), high-Ca alkaline basalts (b) and peridotite xenoliths hosted in low-Ca alkaline basalts (c) in the Nanjing basaltic field. The primitive mantle values are from McDonough and Sun (1995). Fields of MORB and OIB are based on the data from Barnes et al. (2015).

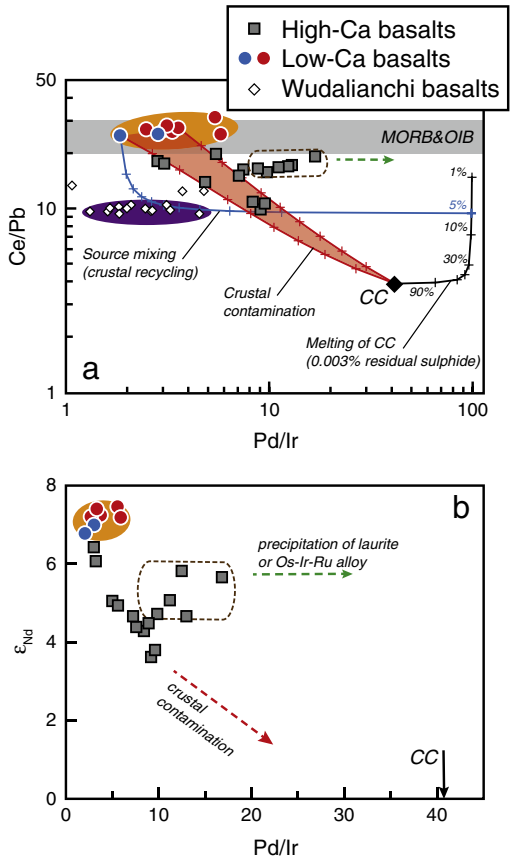

Fig. 7. Variations in Ce/Pb (a) and ε_{Nd}(b) vs. Pd/Ir for Cenozoic alkaline basalts in Nanjing basaltic field. Also shown is the simple batch-melting curve (the black curve) calculated for eclogite. Partition coefficient of clinopyroxene/garnet for Ce, Pb are taken from Klemme et al. (2002). Partition coefficient of sulfide for Pd, Ir are taken from Mungall and Brenan (2014). Partition coefficient of clinopyroxene for Pd, Ir are after Chazey and Neal (2005).Partition coefficients of garnet for Pd, Ir and of sulfide for Ce, Pb are assumed to be zero. The proportions of residual phase during melting of eclogite are assumed to be modal (50% garnet, 49.997 clinopyroxene and 0.003% sulfide). Wudalianchi basalts in eastern China (white diamond) are also shown (Chu et al., 2013). The field of MORB and OIB is after Hofmann et al. (1986), based on their Ce/Pb ratios. Data for CC (continental crust) are from Rudnick and Gao (2003).

of Pd between sulfide and melt is much higher than Cu (Mungall and Brenan, 2014), the sulfide remnant or early-sulfide segregation in the source would produce basaltic melt with high Cu/Pd ratio (Barnes and Maier, 1999; Bennett et al., 2000). During melting in low degree, the basaltic melts would have decreased Pd concentrations and increased Cu/Pd ratios with the increased proportion of sulfide in the residue. Melting of peridotite with variable proportions of residual sulfide in the source can reproduce the high Cu/Pd ratios of low-Ca alkaline basalts. For those high-Ca alkaline basalts (except for samples 08FSLH16 and 08FSLH17), their Cu/Pd ratios (1.1×10^5–4.7×10^5) are significantly higher than those of low-Ca alkaline basalts (0.7×10^5–1.2×10^5), which indicates that a high proportion of residual sulfide is required in the source in order to produce such high Cu/Pd ratios. However, because Pd is extremely compatible in the sulfide (Mungall and Brenan, 2014), increased proportion of residual sulfide would also induce the strong depletion of Pd in the basaltic melt, and cannot reproduce the trend of high-Ca alkaline basalts (Fig. 8). Furthermore, if low-Ca and high-Ca alkaline basalts are generated from a similar sulfide-saturated source, the variation of Cu/Pd ratios should be constant, otherwise their PGEs must be modified by other geological process. In addition, the PGE compositions of low-Ca alkaline basalts are correlated with their Sc concentrations, Hf isotopes and some element ratios (Lu/Hf, Na/Ti and Ca/Al), which are not observed in those high-Ca alkaline basalts (Figs. 4, 5). Obviously, these correlations cannot be produced only by the variable degrees of partial melting. Therefore, the genesis of low-Ca and high-Ca alkaline basalts is complicate, and we will follow this for further discussion.

6.4. Sulfide-saturated AFC process in high-Ca alkaline basalts

Because of obviously low, variable Ce/Pb ratios (9.9–19.2) and ε_{Nd} values (+3.6–+6.4), the influence of crustal component should be considered for the high-Ca alkaline basalts. Previous studies have suggested that the contamination of crustal component might be a possible process to induce the sulfide saturation and the removal of sulfide (Keays and Lightfoot, 2007; Lightfoot and Keays, 2005). The Pd/Ir ratios of high-Ca alkaline basalts are generally correlated with the Ce/Pb ratios and ε_{Nd} values (Fig. 7), which also strongly suggest that the PGE compositions for these basalts are affected by this process. Though contamination of crustal component can occur during ascent (crustal contamination) or in the mantle source (crustal recycling), we prefer the former based on the calculated results. As shown in Fig. 7a, if the crustal components are present in the mantle source, the crust-derived melts would be significantly depleted in PGE for the residue of sulfides, and the slight contamination of such crust-derived melts in the source would not modify the PGE compositions of basaltic magmas remarkably. By comparison, crustal contamination of basaltic magmas can increase the Pd/Ir ratios significantly with the decreased Ce/Pb

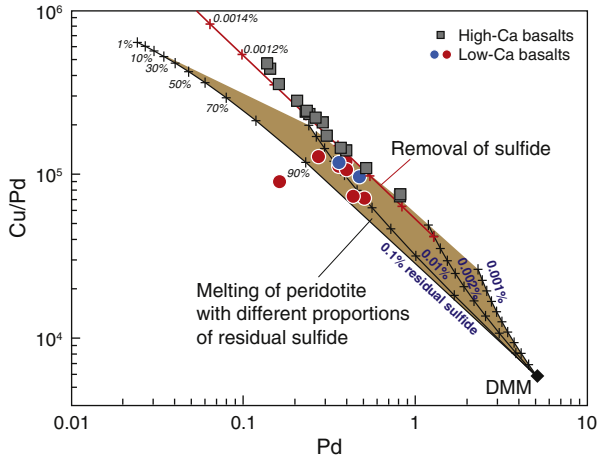

Fig. 8. Variations in Cu/Pd vs. Pd for Cenozoic alkaline basalts in Nanjing basaltic field. Also shown is the simple batch-melting curve (the black curve) calculated for peridotite with residual sulfide. Partition coefficient of olivine, clinopyroxene, orthopyroxene, and garnet for Pd are taken from Chazey and Neal (2005). Partition coefficient of olivine, clinopyroxene, orthopyroxene, and garnet for Cu are taken from Klock and Palme (1988); Hart and Dunn (1993); Klemme et al. (2006) and Yurimoto and Ohtani (1992), respectively. Partition coefficient of sulfide for Pd and Cu are taken from Mungall and Brenan (2014). The proportions of residual phase during melting of eclogite are assumed to be modal (62% olivine, 14.9%–14.999% clinopyroxene, 15% orthopyroxene, 8% garnet and 0.1%–0.001% sulfide). Data for DMM (depleted MORB mantle) are from Salters and Stracke (2004).

ratios because the continental crust show high Pd/Ir ratios (≈41) and low Ce/Pb ratios (≈3.9) (Rudnick and Gao, 2003).

Simple mixing calculations between low-Ca alkaline basalts and the average bulk continental crust (the contamination of 10%–50% crustal material) increase the Pd/Ir ratios from 1.8 to 8.0 with the decreased Ce/Pb ratios (from 24.9 to 9.4), and can reproduce the co-variations of Ce/Pb and Pd/Ir ratios of high-Ca alkaline basalts. Similar proportion of contamination in the mantle source (Fig. 7a) can only slightly increase the Pd/Ir ratios (from 1.8 to 3.0) of basaltic melts. Wudalianchi basalts, whose source has been proposed to be metasomatized by continental crust-derived melts (Chu et al., 2013), are plotted at the line of peridotite-derived melt and continental crust-derived melt. Additionally, in the plots of Cu/Pd vs. Pd (Fig. 8), we calculate the removal of sulfide from the sulfide-residual mantle-derived basaltic magma during ascent. Few amounts of removal of sulfide can well reproduce the variations of Cu/Pd ratios and Pd concentrates of high-Ca alkaline basalts. Therefore, we propose that crustal contamination plays an important role in the fractionation of IPGE and PPGE of high-Ca alkaline basalts, and the high Cu/Pd ratios of these basalts are also induced by the removal of sulfide during this process. Samples 08FSLH16 and 08FSLH17 have the highest ε_{Nd} values (+6.0–+6.4) among high-Ca basalts, indicating that they should undergo the minimum influence of crustal contamination. Their high Pd contents and low Cu/Pd ratios (7.3×10^4–7.5×10^4) relative to other high-Ca basalts, which indicate that they have undergone small degree removal of sulfide, again support that the PGEs of high-Ca basalts are affected by such sulfide-saturated AFC process.

Furthermore, in the plot of Ce/Pb vs. Pd/Ir (Fig. 7), some high-Ca alkaline basalts have deviated from the crustal contamination trend, and for a given Ce/Pb ratio or ε_{Nd} value, these samples have obviously higher Pd/Ir ratios than other high-Ca alkaline basalts. This indicates an additional geological process to intensify the fractionation of IPGE from PPGE. During the early stages of fractional crystallization, the precipitation of laurite or Ru–Os–Ir alloys formed by IPGE (e.g., Amossé et al., 1990, Capobianco and Drake, 1990), which might be enclosed in olivine or chromite (Stockman, 1984), would give rise to the IPGE depletion and PPGE enrichment effectively in magmas. Such phenomena are also revealed in some Permian Emeishan flood basalts in southwestern China (Qi and Zhou, 2008; Wang et al., 2014) and layered komatiite flows from Belingwe greenstone belt in Zimbabwe (Zhou, 1994). Therefore, we propose that the increased Pd/Ir ratios of these high-Ca alkaline basalts are induced by the fractionation of laurite or Ru–Os–Ir alloys within olivine.

6.5. Xenolith–magma interaction in low-Ca alkaline basalts

For low-Ca alkaline basalts, some samples show negative anomalies of Pt in a primitive mantle-normalized chalcophile element diagram (Fig. 6a), which may initially be thought to relate to the contamination of peridotite xenolith fragments. However, except for Pt, peridotite fragments have similar concentrations of other PGEs (Fig. 6c). Previous studies also suggest that such peridotite fragments have low Na/Ti and

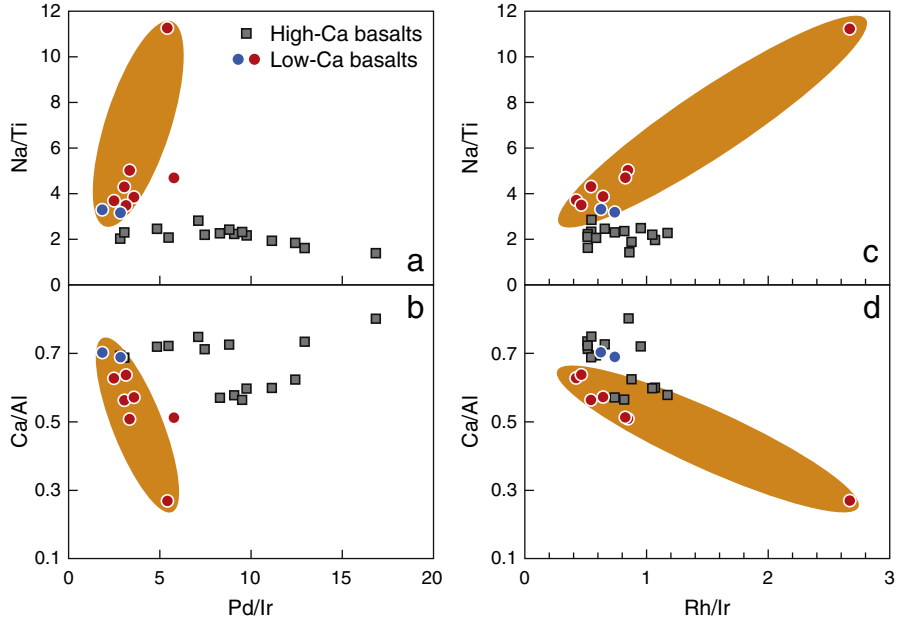

Fig. 9. Variations in Na/Ti vs. Pd/Ir (a), Ca/Al vs. Pd/Ir (b), Na/Ti vs. Rh/Ir (c), and Ca/Al vs. Rh/Ir (d) for Cenozoic alkaline basalts in the Nanjing basaltic field.

high Ca/Al ratios (Zeng et al., 2013). Obviously, even though the contamination of the peridotite fragments has affected the PGEs of the basalts, an additional process is still required to explain the good correlations between PGEs/PGE ratios and elemental ratios (Na/Ti and Ca/Al ratios). Therefore, the interaction between basaltic magmas and peridotite xenoliths is proposed to be involved in the alteration of the host basalts (Zeng et al., 2013).

During the ascent of basaltic magmas, the peridotite xenoliths underwent low-pressure melting, and the host magmas were contaminated by mantle xenoliths-derived melts, transforming the magmas into the low-Ca alkaline basalts. Such interaction would decrease the MgO, CaO, Sc contents and Lu/Hf, Ca/Al ratios, and increase Na/Ti ratios and ε_{Hf} values of the host basalts. However, whether this process can also affect the PGE compositions of host basalts is unknown. As shown in Figs. 3, 4, 5, the PGE compositions of low-Ca alkaline basalts are well correlated with MgO, Sc contents, element ratios (Lu/Hf, Na/Ti and Ca/Al) and Hf isotopes. Additionally, there are good correlations between PGE ratios (Pd/Ir and Rh/Ir) and those element ratios (Na/Ti and Ca/Al) which are sensitive to xenolith-magma interaction (Fig. 9). Therefore, we suggest that xenolith–magma interaction modifies the PGE compositions of low-Ca alkaline basalts.

In order to evaluate whether such xenolith–magma can modify the PGE compositions of basaltic magma, we calculate the PGE compositions of melts according to the model of Zeng et al. (2013). As shown in Fig. 10, melting of peridotite xenolith in low degree can produce the melts with high Pd/Ir ratios. For a given melting degree, the Pd/Ir ratios of melts are decreased with the increased proportion of residual sulfide in the peridotite xenolith. Only tiny amounts (0.003%) of residual sulfide can reproduce the compositional variations of low-Ca alkaline basalts. Because of the retention of sulfide in the peridotite xenolith, the PGE compositions of peridotite-derived melts should be depleted, which is accordant with the variations in the plots of PGEs vs. MgO contents (Fig. 3).Additionally, the PGE compositions of peridotite xenoliths in low-Ca alkaline basalts show no obviously difference between the core and margin (Fig. 6c), again suggest that the PGEs are still retained in the residual sulfide in the peridotite xenoliths.

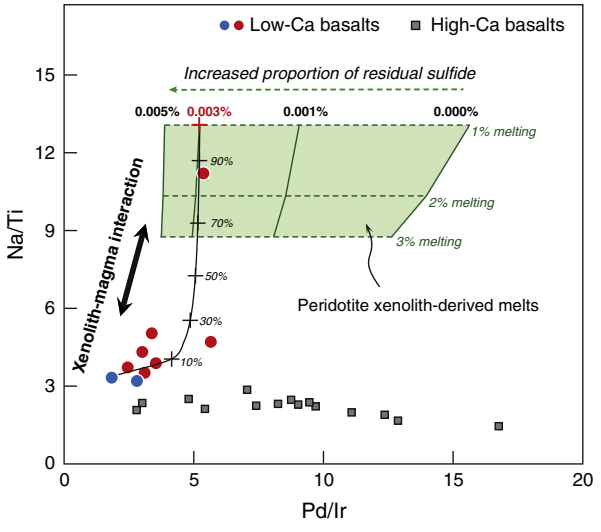

Fig. 10. Variations in Na/Ti vs. Pd/Ir for Cenozoic alkaline basalts in Nanjing basaltic field. Also shown is the simple batch-melting curves (the green curves) calculated for peridotite xenolith. Partition coefficient of sulfide for Pd, Ir are taken from Mungall and Brenan (2014). Partition coefficient of olivine and clinopyroxene for Pd, Ir are after Chazey and Neal (2005). Partition coefficient of spinel for Pd, Ir are taken from Righter et al. (2004). Partition coefficients of orthopyroxene for Pd, Ir are assumed to be zero. Partition coefficients of orthopyroxene for Na, Ti are taken from Frei et al. (2009). Partition coefficients of olivine and clinopyroxene for Ti are taken from Adam and Green (2006). Partition coefficients of olivine and clinopyroxene for Na are taken from Borisov et al. (2008) and Blundy et al. (1995), respectively. Partition coefficients of spinel for Ti are taken from Righter et al. (2006). The Na and Ti for starting materials are after Zeng et al. (2013). The residual mineral modal compositions are based on margin of peridotite xenolith (69.997% olivine, 15% clinopyroxene, 14% orthopyroxene, 1% spinel and 0.003% sulfide).

7. Conclusions

(1) Both low-Ca and high-Ca alkaline basalts from Nanjing basaltic field are highly depleted in PGEs relative to Ni and Cu and were derived from sulfide-saturated, partial melts of the mantle source.
(2) High-Ca alkaline basalts have highly variable Cu/Pd and Pd/Ir ratios and have undergone sulfide-saturated assimilation-fractionation crystallization (SAFC). Some high-Ca alkaline basalts deviate from the trend of crustal contamination, which can be explained by the fractionation of laurite or Ru–Os–Ir alloys with olivine.
(3) PGE compositions of low-Ca alkaline basalts are primarily controlled by xenolith-magma interaction.

Supplementary data to this article can be found online at http://dx.doi.org/10.1016/j.lithos.2016.04.032.

Acknowledgements

We are grateful to Ye Liu, Yue-Heng Yang, and Wei Pu for their technical support. Greg A.Valentine, Xun Yu and Xia-Yu Chen attended the field investigations of this study. We appreciate the thoughtful and constructive reviews provided by Editor Sun-Lin Chung and the two anonymous reviewers. This work was supported by the Research Grant Council of Hong Kong (HKU706413P), the National Basic Research Program of China (2012CB416701), the National Natural Science Foundation of China (grant 41430208, 41202039) and a research grant from the State Key Laboratory for Mineral Deposits Research, Nanjing University (grant ZZKT-201320).

References

Adam, J., Green, T., 2006. Trace element partitioning between mica- and amphibole-bearing garnet lherzolite and hydrous basanitic melt: 1. Experimental results and the investigation of controls on partitioning behavior. Contributions to Mineralogy and Petrology 152, 1–17.
Amossé, J., Allibert, M., Fischer, W., Piboule, M., 1990. Experimental study of the solubility of platinum and iridium in basic silicate melts—implications for the differentiation of platinum-group elements during magmatic processes. Chemical Geology 81, 45–53.
Anhui Institute of Geological Survey, 1977. 1:200000 Geological Map, Nanjing Scope.
Barnes, S.-J., Maier, W., 1999. The fractionation of Ni, Cu and the noble metals in silicate and sulphide liquids. Geological Association of Canada Short Course Notes 13, 69–106.
Barnes, S.J., Mungall, J.E., Maier, W.D., 2015. Platinum group elements in mantle melts and mantle samples. Lithos 232, 395–417.
Bennett, V.C., Norman, M.D., Garcia, M.O., 2000. Rhenium and platinum group element abundances correlated with mantle source components in Hawaiian picrites: sulphides in the plume. Earth and Planetary Science Letters 183, 513–526.
Bezmen, N., Asif, M., Brügmann, G., Romanenko, I., Naldrett, A., 1994. Distribution of Pd, Rh, Ru, Ir, Os, and Au between sulfide and silicate metals. Geochimica et Cosmochimica Acta 58, 1251–1260.
Blundy, J.D., Falloon, T.J., Wood, B.J., Dalton, J.A., 1995. Sodium partitioning between clinopyroxene and silicate melts. Journal of Geophysical Research 100, 15501–15515.
Borisov, A., Pack, A., Kropf, A., Palme, H., 2008. Partitioning of Na between olivine and melt: an experimental study with application to the formation of meteoritic Na_2O-rich chondrule glass and refractory forsterite grains. Geochimica et Cosmochimica Acta 72, 5558–5573.
Capobianco, C.J., Drake, M.J., 1990. Partitioning of ruthenium, rhodium, and palladium between spinel and silicate melt and implications for platinum group element fractionation trends. Geochimica et Cosmochimica Acta 54, 869–874.
Carlson, R.W., Lugmair, G.W., Macdougall, J.D., 1981. Columbia River volcanism: the question of mantle heterogeneity or crustal contamination. Geochimica et Cosmochimica Acta 45, 2483–2499.
Chazey, W.J., Neal, C.R., 2005. Platinum-group element constraints on source composition and magma evolution of the Kerguelen Plateau using basalts from ODP Leg 183. Geochimica et Cosmochimica Acta 69, 4685–4701.
Chu, Z.-Y., Harvey, J., Liu, C.-Z., Guo, J.-H., Wu, F.-Y., Tian, W., Zhang, Y.-L., Yang, Y.-H., 2013. Source of highly potassic basalts in northeast China: evidence from Re–Os, Sr–Nd–Hf isotopes and PGE geochemistry. Chemical Geology 357, 52–66.

Crocket, J.H., Paul, D.K., 2004. Platinum-group elements in Deccan mafic rocks: a comparison of suites differentiated by Ir content. Chemical Geology 208, 273–291.
Frei, D., Liebscher, A., Franz, G., Wunder, B., Klemme, S., Blundy, J., 2009. Trace element partitioning between orthopyroxene and anhydrous silicate melt on the lherzolite solidus from 1.1 to 3.2 GPa and 1,230 to 1,535 °C in the model system Na_2O–CaO–MgO–Al_2O_3–SiO_2. Contributions to Mineralogy and Petrology 157, 473–490.
Govindaraju, G., 1994. Compilation of working values and sample description for 383 geostandards. Geostandards Newslett 18, 1–158.
Hart, S.R., Dunn, T., 1993. Experimental cpx/melt partitioning of 24 trace elements. Contributions to Mineralogy and Petrology 113, 1–8.
Hofmann, A.W., 1997. Mantle geochemistry: the message from oceanic volcanism. Nature 385, 219–229.
Hofmann, A.W., 2003. Sampling mantle heterogeneity through oceanic basalts: isotopes and trace elements. In: Holland, H.D., Turekian, K.K. (Eds.), Treatise on Geochemistry. Elsevier, Amsterdam, pp. 61–102.
Hofmann, A.W., Jochum, K.P., Seufert, M., White, W.M., 1986. Nb and Pb in oceanic basalts: new constraints on mantle evolution. Earth and Planetary Science Letters 79, 33–45.
Huang, X.-W., Zhou, M.-F., Wang, C.Y., Robinson, P.T., Zhao, J.-H., Qi, L., 2013. Chalcophile element constraints on magma differentiation of Quaternary volcanoes in Tengchong, SW China. Journal of Asian Earth Sciences 76, 1–11.
Jiangsu Institute of Geological Survey, 1978. 1:200000 Geological Map, Xuyi Scope.
Keays, R., Lightfoot, P., 2007. Siderophile and chalcophile metal variations in Tertiary picrites and basalts from West Greenland with implications for the sulphide saturation history of continental flood basalt magmas. Mineralium Deposita 42, 319–336.
Keays, R.R., 1995. The role of kamatitic and picritic magmatism and S-saturation in the formation of ore-deposits. Lithos 34, 1–18.
Klemme, S., Blundy, J.D., Wood, B.J., 2002. Experimental constraints on major and trace element partitioning during partial melting of eclogite. Geochimica et Cosmochimica Acta 66, 3109–3123.
Klemme, S., Günther, D., Hametner, K., Prowatke, S., Zack, T., 2006. The partitioning of trace elements between ilmenite, ulvospinel, armalcolite and silicate melts with implications for the early differentiation of the moon. Chemical Geology 234, 251–263.
Klock, W., Palme, H., 1988. Partitioning of siderophile and chalcophile elements between sulfide, olivine, and glass in a naturally reduced basalt from Disko Island, Greenland. In: Ryder, G. (Ed.), Proceedings of Lunar and Planetary Science Conference. Pergamon, New York, pp. 471–483.
Koszowska, E., Wolska, A., Zuchiewicz, W., Cuong, N.Q., Pécskay, Z., 2007. Crustal contamination of Late Neogene basalts in the Dien Bien Phu Basin, NW Vietnam: some insights from petrological and geochronological studies. Journal of Asian Earth Sciences 29, 1–17.
Li, S.G., Jagoutz, E., Chen, Y.Z., Li, Q.L., Xiao, Y.L., 1999. Sm/Nd, Rb/Sr, and $^{40}Ar/^{39}Ar$ isotopic systematics of the ultrahigh-pressure metamorphic rocks in the Dabie–Sulu belt, Central China: a retrospective view. International Geology Review 41, 1114–1124.
Lightfoot, P.C., Keays, R.R., 2005. Siderophile and chalcophile metal variations in flood basalts from the Siberian Trap, Noril'sk Region: implications for the origin of the Ni–Cu–PGE sulfide ores. Economic Geology 100, 439–462.
Liu, R.X., Chen, W.J., Sun, J.Z., Li, D.M., 1992. The K–Ar age and tectonic environment of Cenozoic volcanic rock in China. In: Liu, R.X. (Ed.), The Age and Geochemistry of Cenozoic Volcanic Rock in China. Seismic Press, Beijing, pp. 1–43.
Lustrino, M., Fedele, L., Melluso, L., Morra, V., Ronga, F., Geldmacher, J., Duggen, S., Agostini, S., Cucciniello, C., Franciosi, L., Meisel, T., 2013. Origin and evolution of Cenozoic magmatism of Sardinia (Italy). A combined isotopic (Sr–Nd–Pb–O–Hf–Os) and petrological view. Lithos 180, 138–158.
McDonough, W.F., Sun, S.S., 1995. The composition of the Earth. Chemical Geology 120, 223–253.
Meisel, T., Moser, J., 2004. Reference materials for geochemical PGE analysis: new analytical data for Ru, Rh, Pd, Os, Ir, Pt and Re by isotope dilution ICP-MS in 11 geological reference materials. Chem. Geol. 208, 319–338.
Momme, P., Oskarsson, N., Keays, R.R., 2003. Platinum-group elements in the Icelandic rift system: melting processes and mantle sources beneath Iceland. Chemical Geology 196, 209–234.
Mungall, J.E., Brenan, J.M., 2014. Partitioning of platinum-group elements and Au between sulfide liquid and basalt and the origins of mantle–crust fractionation of the chalcophile elements. Geochimica et Cosmochimica Acta 125, 265–289.
Niu, Y.L., 2008. The origin of alkaline lavas. Science 320, 883–884.
O'Reilly, S.Y., Zhang, M., 1995. Geochemical characteristics of lava-field basalts from eastern Australia and inferred sources: connections with the subcontinental lithospheric mantle? Contributions to Mineralogy and Petrology 121, 148–170.
Peach, C., Mathez, E.A., Keays, R.R., Reeves, S., 1994. Experimentally determined sulfide melt-silicate melt partition coefficients for iridium and palladium. Chemical Geology 117, 361–377.
Prytulak, J., Elliott, T., 2007. TiO_2 enrichment in ocean island basalts. Earth and Planetary Science Letters 263, 388–403.
Pu, W., Gao, J.F., Zhao, K.D., Lin, H.F., Jiang, S.Y., 2005. Separation method of Rb–Sr, Sm–Nd using DCTA and HIBA. Journal of Nanjing University (Natural Sciences) 41, 445–450.
Qi, L., Zhou, M.-F., 2008. Platinum-group elemental and Sr-Nd-Os isotopic geochemistry of Permian Emeishan flood basalts in Guizhou Province, SW China. Chemical Geology 248, 83–103.
Qi, L., Zhou, M.-F., Wang, C.Y., 2004. Determination of low concentrations of platinum group elements in geological samples by ID-ICP-MS. J. Anal. At. Spectrom. 19, 1335–1339.
Qi, L., Gao, J.F., Huang, X.W., Hu, J., Zhou, M.F., Zhong, H., 2011. An improved digestion technique for determination of platinum group elements in geological samples. Journal of Analytical Atomic Spectrometry 26, 1900–1904.
Rehkamper, M., Halliday, A.N., Fitton, J.G., Lee, D.C., Wieneke, M., Arndt, N.T., 1999. Ir, Ru, Pt, and Pd in basalts and komatiites: new constraints for the geochemical behavior of the platinum-group elements in the mantle. Geochimica et Cosmochimica Acta 63, 3915–3934.
Righter, K., Campbell, A.J., Humayun, M., Hervig, R.L., 2004. Partitioning of Ru, Rh, Pd, Re, Ir, and Au between Cr-bearing spinel, olivine, pyroxene and silicate melts1. Geochimica et Cosmochimica Acta 68, 867–880.
Righter, K., Leeman, W.P., Hervig, R.L., 2006. Partitioning of Ni, Co and V between spinel-structured oxides and silicate melts: importance of spinel composition. Chemical Geology 227.
Rudnick, R.L., Gao, S., 2003. Composition of the continental crust. In: Holland, H.D., Turekian, K.K. (Eds.), Treatise on Geochemistry. Elsevier, Amsterdam, pp. 1–64.
Salters, V.J.M., Stracke, A., 2004. Composition of the depleted mantle. Geochemistry, Geophysics, Geosystems 5. http://dx.doi.org/10.1029/2003gc000597.
Seitz, H.M., Keays, R.R., 1997. Platinum group element segregation and mineralization in a Noritic ring complex formed from Proterozoic siliceous high magnesium basalt magmas in the Vestfold Hills, Antarctica. Journal of Petrology 38, 703–725.
Stockman, H., 1984. Electron-microprobe characterization of minute platinum-group mineral inclusions: limits on accuracy. Scanning Electron Microscopy 3, 1097–1109.
Tang, Y.J., Zhang, H.F., Ying, J.F., 2006. Asthenosphere–lithospheric mantle interaction in an extensional regime: implication from the geochemistry of Cenozoic basalts from Taihang Mountains, North China Craton. Chemical Geology 233, 309–327.
Wang, C.Y., Zhou, M.-F., Qi, L., 2010. Origin of extremely PGE-rich mafic magma system: an example from the Jinbaoshan ultramafic sill, Emeishan large igneous province, SW China. Lithos 119, 147–161.
Wang, C.Y., Zhou, M.-F., Yang, S., Qi, L., Sun, Y., 2014. Geochemistry of the Abulangdang intrusion: cumulates of high-Ti picritic magmas in the Emeishan large igneous province, SW China. Chemical Geology 378–379, 24–39.
Weis, D., Kieffer, B., Hanano, D., Nobre Silva, I., Barling, J., Pretorius, W., Maerschalk, C., Mattielli, N., 2007. Hf isotope compositions of U.S. Geological Survey reference materials. Geochemistry, Geophysics, Geosystems 8. http://dx.doi.org/10.1029/2006gc001473.
Willbold, M., Stracke, A., 2010. Formation of enriched mantle components by recycling of upper and lower continental crust. Chemical Geology 276, 188–197.
Xu, Y.G., Ma, J.L., Frey, F.A., Feigenson, M.D., Liu, J.F., 2005. Role of lithosphere–asthenosphere interaction in the genesis of Quaternary alkali and tholeiitic basalts from Datong, western North China Craton. Chemical Geology 224, 247–271.
Yang, Y.H., Zhang, H.F., Chu, Z.Y., Xie, L.W., Wu, F.Y., 2010. Combined chemical separation of Lu, Hf, Rb, Sr, Sm and Nd from a single rock digest and precise and accurate isotope determinations of Lu–Hf, Rb–Sr and Sm–Nd isotope systems using Multi-Collector ICP-MS and TIMS. International Journal of Mass Spectrometry 290, 120–126.
Yurimoto, H., Ohtani, E., 1992. Element partitioning between majorite and liquid: a secondary ion mass spectrometric study. Geophysical Research Letters 19, 17–20.
Zeng, G., Chen, L.-H., Hu, S.-L., Xu, X.-S., Yang, L.-F., 2013. Genesis of Cenozoic low-Ca alkaline basalts in the Nanjing basaltic field, eastern China: the case for mantle xenolith–magma interaction. Geochemistry, Geophysics, Geosystems 14, 1660–1677.
Zhao, D.S., Xiao, Z.Y., Wang, Y.T., 1983. Petrological characteristics and genesis of the Cenozoic volcanic rocks in Tancheng–Lujiang fault belt and the adjacent areas. Acta Geologica Sinica 2, 128–141.
Zheng, Y.F., Fu, B., Gong, B., Li, L., 2003. Stable isotope geochemistry of ultrahigh pressure metamorphic rocks from the Dabie–Sulu orogen in China: implications for geodynamics and fluid regime. Earth Science Reviews 62, 105–161.
Zheng, Y.F., Zhou, J.B., Wu, Y.B., Zhao, Z.F., 2005. Low-grade metamorphic rocks in the Dabie–Sulu orogenic belt: a passive-margin accretionary wedge deformed during continent subduction. International Geology Review 47, 851–871.
Zhou, M.F., 1994. PGE distribution in 2.7-Ga layered komatiite flows from the Belingwe greenstone belt, Zimbabwe. Chemical Geology 118, 155–172.